

Advanced Material Design and Engineering for Water-Based Evaporative Cooling

Renyuan Li, Wenbin Wang, Yifeng Shi, Chang-ting Wang, and Peng Wang*

Water-based evaporative cooling is emerging as a promising technology to provide sustainable and low-cost cold to alleviate the rising global cooling demand. Given the significant and fast progress made in recent years, this review aims to provide a timely overview on the state-of-the-art material design and engineering in water-based evaporative cooling. The fundamental mechanisms and major components of three water-based evaporative cooling processes are introduced, including direct evaporative cooling, cyclic sorption-driven liquid water evaporative cooling (CSD-LWEC), and atmospheric water harvesting-based evaporative cooling (AWH-EC). The distinctive requirements on the sorbent materials in CSD-LWEC and AWH-EC are highlighted, which helps synthesize the literature information on the advanced material design and engineering for the purpose of improving cooling performance. The challenges and future outlooks on further improving the water-based evaporative cooling performance are also provided.

accessibility, and people living in the impoverished regions are unable to enjoy the advanced cooling technologies due to the lack of stable electricity supply.^[10,11]

From a scientific point of view, cold can be generated by heat exchange and thermal absorption.^[12] Active heat exchange generates cold by transferring heat from low to high temperature region driven by high-grade energy (e.g., electricity) while passive heat exchange produces cold by transferring heat from high to low temperature region in the absence of external energy input, with sky cooling being one example.^[13–18] However, its nature of being passive radiative cooling inevitably makes it have a low intrinsic thermodynamic cooling power ceiling of $\approx 160 \text{ W m}^{-2}$,^[19] and thus necessitates a large land footprint for its application. On

the other hand, thermal absorption generates cold by taking advantage of the endothermic process such as dissolving.^[20,21] The dissolution-based cooling process employs specific chemical compounds, such as ammonium nitrate, that absorbs heat during its dissolution. However, it requires large amount of energy to recycle the dissolved chemicals from its solution. The active thermal absorption is by far the most commonly used cooling process in domestic, commercial, and industrial activities mainly due to its high cooling power.^[22] For example, compression-based cooling (e.g., air conditioning and refrigeration) generates cold by evaporating refrigerant and circulating refrigerant via gas compression, achieving superior energy efficiency and coefficient of performance ($\text{COP} > 2$).^[23] However, it is very electricity-intensive, resulting in cooling being a large share of the global electricity consumer and greenhouse gas emitter.^[24]


In this context, passive cooling is emerging, among which passive water-based evaporative cooling using water as refrigerant is attracting significant attentions.^[25–27] Due to the extensive network of the hydrogen bonds formed between the neighboring hydrogen and oxygen atoms of the adjacent water molecules, water has the highest enthalpy of vaporization among all room temperature liquids.^[28] As a result, water-based evaporative cooling shows the advantages of higher cooling power due to its high evaporation enthalpy compared to other evaporative cooling technology. Moreover, it has a broader application scenario, which could meet various application demands, such as house cooling, electronic device cooling, industrial cooling, as well as food storage. In addition, water is nontoxic, safe, and easily accessible. Therefore, phase change of water (i.e., evaporation) is an effective, green, and convenient way to produce cold.

1. Introduction

Cooling has a wide range of end-use applications as it can regulate the temperature of spaces and objects for building temperature control, food storage, and device heat dissipation.^[1–4] However, global cooling demand is set to roar as a result of the ongoing global warming, ever-growing global population, and the steadily improving life standards.^[5–7] The prevailing cooling technologies, such as air conditioning and refrigeration, rely on electricity as the energy source. It has been estimated that cooling accounts for 15% of global electricity consumption and produces 10% of the global greenhouse gas emission.^[8,9] Furthermore, their high electricity consumption limits their

R. Li, W. Wang, Y. Shi, P. Wang
Water Desalination and Reuse Center
Division of Biological and Environmental Science and Engineering
King Abdullah University of Science and Technology
Thuwal 23955-6900, Saudi Arabia
E-mail: peng.wang@kaust.edu.sa

C.-t. Wang, P. Wang
Department of Civil and Environmental Engineering
the Hong Kong Polytechnic University
Hong Kong 999077, China

 The ORCID identification number(s) for the author(s) of this article can be found under <https://doi.org/10.1002/adma.202209460>.

© 2023 The Authors. Advanced Materials published by Wiley-VCH GmbH. This is an open access article under the terms of the Creative Commons Attribution License, which permits use, distribution and reproduction in any medium, provided the original work is properly cited.

DOI: 10.1002/adma.202209460

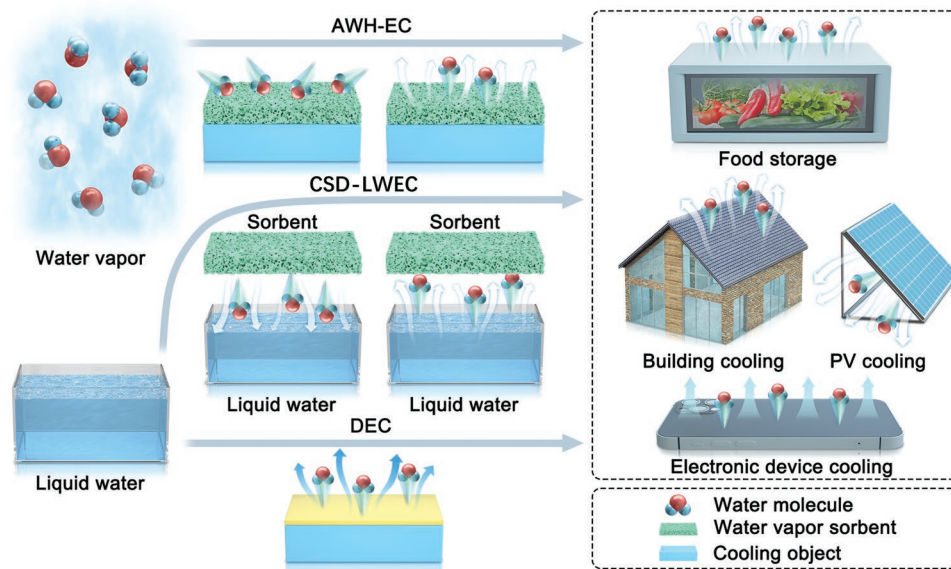


Figure 1. Schematic illustration of three major water-based evaporative cooling processes.

Water-based evaporative cooling can be achieved through three different approaches (**Figure 1**): direct evaporative cooling (DEC), cyclic sorption-driven liquid water evaporative cooling (CSD-LWEC), and atmospheric water harvesting-based evaporative cooling (AWH-EC). Direct evaporative cooling is the embryonic form of the advanced evaporative cooling processes. Heat is extracted largely from liquid water to overcome the enthalpy of vaporization of water and the liquid water, which is a sacrificial working fluid in this case, is cooled down accordingly.^[29–31] Consequently, its application scenario is limited due to the consumption of large amounts of liquid water. To this end, CSD-LWEC or AWH-EC either recycle the generated vapor^[32–34] or harvest vapor from ambient air by using easily regenerable water vapor sorbents to reduce its reliance over bulk water.^[35–37] It is worth pointing out, when sorbing water vapor, hygroscopic materials maintain a solid-like form while deliquescent ones form aqueous solution.^[38] In a typical CSD-LWEC system, the water evaporation rate and thus the cooling power is promoted by the enhanced water vapor pressure gradient between the liquid water and sorbent in comparison to that in DEC, and the sorbent can be regenerated by utilizing low-grade waste heat (e.g., solar heat and industrial waste heat).^[39–41] On the other hand, AWH-EC emerged only in the past two years.^[35,42,43] The AWH-EC does not require liquid water supply, is flexible with the device dimension, and represents a new avenue of water-based evaporative cooling.

Since in CSD-LWEC and AWH-EC, water vapor sorbent is a key component, a thorough understanding to fundamental sorbent properties, their water sorption–desorption cycles, the ways of modulating the interactions between water and sorbents, along with the cooling system design, could lead to a rational enhancement of their cooling performance. In this review, we seek to highlight and discuss the recent development on water-based evaporative cooling with a clear focus on advanced sorbent materials and system designs. This review first introduces the fundamentals of evaporative cooling pro-

cess, followed by the materials-enabled advanced direct evaporative cooling. The distinctive sorbent material properties of CSD-LWEC and AWH-EC are then critically synthesized based on the literature information. The review concludes by highlighting the challenges and future opportunities in order to make the water-based evaporative cooling a significant contributor to the global sustainability.

2. Direct Evaporative Cooling That Consumes Liquid Water

2.1. Overview of Direct Evaporative Cooling

People in Ancient India discovered rapid evaporation at night could cool water in clay pots, leading to the formation of ice. People in Ancient Greece cooled rooms by hanging wet mats in front of the windows. However, these ancient methods usually show an unsatisfactory cooling efficiency when compared to the total energy dissipated from the liquid water during the evaporation. This is because that evaporation only takes place at the water/air interface, and the cooling effect is difficult to be delivered to the cooling object other than the bulk water.

Conventional direct evaporative cooling (DEC) addresses this problem by utilizing specific medium (e.g., air or water) or system (e.g., cooling tower) for a better heat exchange efficiency.^[29,30] The removal of waste heat from the industrial process is through circulated water stream across hot surface, relocating the energy to the atmosphere by exposing the heated water to the ambient for heat exchange and evaporative cooling. This process demonstrates a high cooling power due to the high latent heat and specific heat capacity of water, and consumes electricity mostly in the water circulation process. **Figure 2a** shows the basic working principles of conventional DEC system, in which the ambient air is first chilled as a result of water evaporation when passing through the wet pad, and

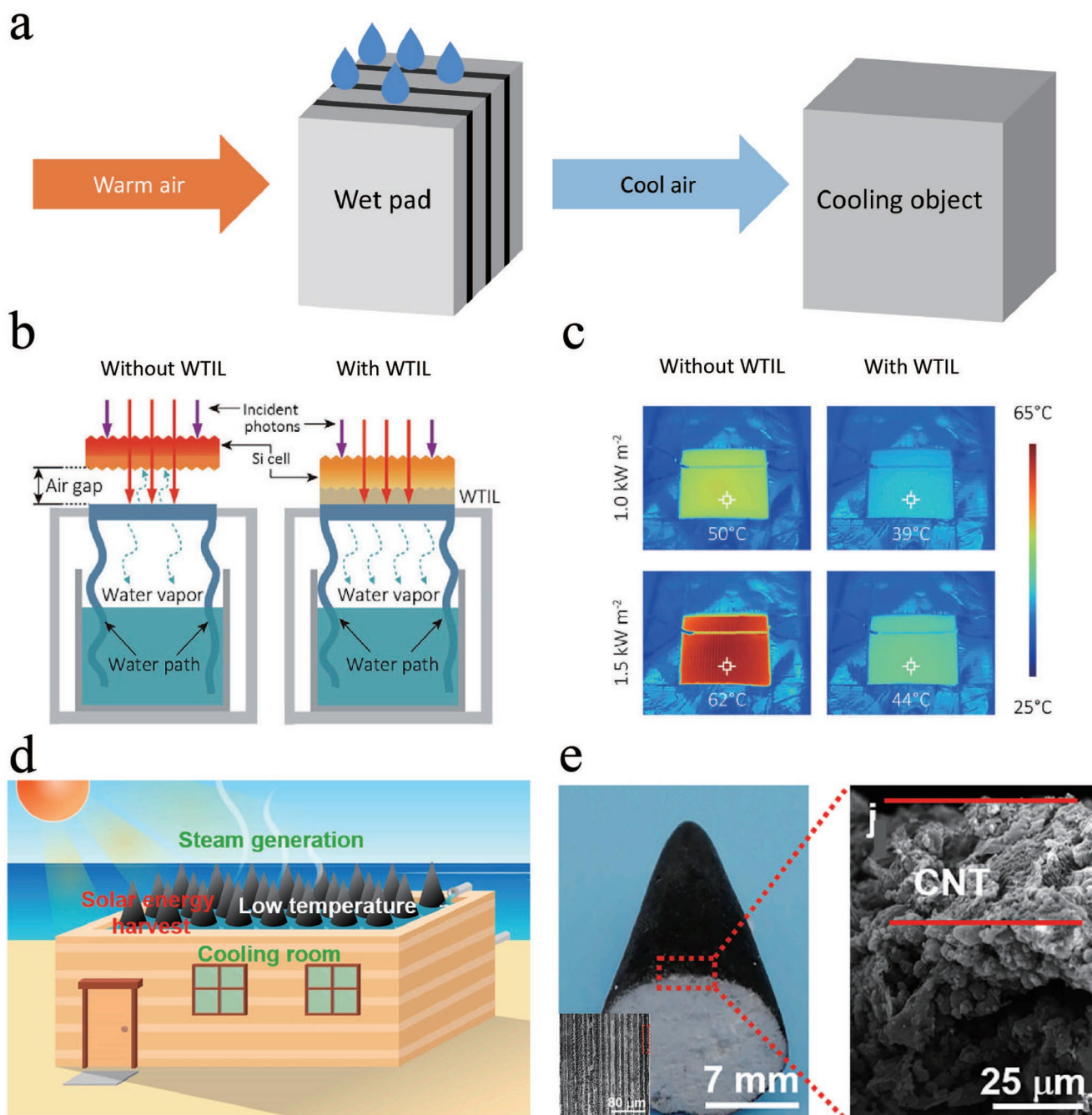


Figure 2. Structures and materials for direct evaporative cooling. a) Schematic illustration of typical direct evaporative cooling system. Reproduced with permission.^[44] Copyright 2021, Elsevier. b) Schematic of IEC with and without water-proof thermal interconnecting layer (WTIL). c) IR images of the solar cell working with and without WTIL. b,c) Reproduced with permission.^[60] Copyright 2019, Elsevier. d) Schematic illustration of a conical aerogel evaporative cooling system for household cooling with simultaneous solar steam generation. e) Picture and SEM image of the conical aerogel (inset: SEM image of the longitudinal section of the conical aerogel). d,e) Reproduced with permission.^[62] Copyright 2021, Elsevier

then used to reduce the temperature of the cooling object.^[44] It is undeniable that great progress has been made during the past centuries in developing advanced wet pad and designing highly efficient evaporative cooling system. However, heat relocation in the conventional DEC system is an indirect process where heat must be transported by water from the hot surface before being exposed and rejected to the ambient air, which potentially reduces its energy efficiency. Conventional DEC is

believed uneconomical at small scale application also due to its complicated configuration.^[45–47]

In light of these concerns in the conventional DEC, in recent years, interfacial evaporative cooling (IEC) is emerging as an advanced DEC process, and is considered a significant milestone of the water-based cooling process. IEC is a direct heat relocation process where an evaporator is attached to the cooling object (e.g., solar cell, thermoelectric generator)^[35,43,48]

and liquid water is delivered to the evaporator surface by a combined capillary and transpiration effect.^[49] In the early stage of IEC development, the evaporator was mainly configured as 2D structure to conveniently attach to the flat surfaces of the cooling objects. This simple configuration results in better stability of the cooling system, but leads to its limited cooling power due to the limited evaporation surface area. The emerging 3D cooling structure is considered one of the most important landmark achievements of the IEC, which significantly increases the evaporation surface area, and introduces energy exchange with the surrounding ambience to facilitate water evaporation and thus achieves better cooling performance.

Due to the low thermal resistance of the evaporator, the cooling effect generated at the water/air interface can be efficiently delivered to the cooling object by thermal conduction. Moreover, IEC is compatible with various types of source water, such as seawater, wastewater, brackish water, brine, which broadens its application scenarios.^[50]

For IEC, the cooling power can be calculated as follows:

$$q_{\text{cool}} = Jh_{\text{lv}} \quad (1)$$

where q_{cool} is cooling power (W m^{-2}), J is the evaporation rate ($\text{kg m}^{-2} \text{h}^{-1}$), h_{lv} is the enthalpy of vaporization of pure water (kJ kg^{-1}). As seen, the cooling power is proportional to the evaporation rate. Therefore, enhancing the evaporation rate is of significance in improving the cooling performance of evaporative cooling. In this section, we discuss how the material engineering promotes the evaporation rate and cooling performance in IEC.

2.2. Materials for IEC

In IEC, two strategies are typically adopted to increase the evaporation rate: reducing enthalpy of vaporization^[51–53] and creating more water/air interface.^[54–56] Reducing the enthalpy of vaporization by developing hydrophilic hydrogel materials would increase the evaporation rate, but has limited effect on the final cooling power while counterproductively consuming more water. In contrast, creating more water/air interface is preferable for evaporative cooling, which could render a high evaporation rate with low surface temperature. Over the past years, the designs of the IEC evaporator underwent the structure evolution from 2D to 3D ones.^[51,57,58] Initially, 2D evaporator with high thermal conductivity was developed. For example, Zhu et al. prepared a water-proof thermal interconnecting layer (WTIL), which allowed the evaporator to be attached to the solar cell and ensured effective transfer of the thermalization energy from the top solar cell to the bottom 2D evaporator (Figure 2b).^[59] Due to the high thermal conductivity of WTIL ($0.98 \text{ W m}^{-1} \text{ K}^{-1}$), the solar cell temperature could be reduced by $11 \text{ }^\circ\text{C}$ with an evaporation rate of $0.8 \text{ kg m}^{-2} \text{ h}^{-1}$. Wang et al. designed a very thin evaporative crystallizer (thickness of 0.8 mm) beneath a photovoltaic-membrane distillation system to dissipate the water condensation heat, which indirectly cooled the solar cell by $15 \text{ }^\circ\text{C}$ (Figure 2c).^[60] Agyekum et al. applied a water-tank-connected wick mesh at the rear side of a PV panel and achieved a temperature drop (i.e., the tem-

perature differences between the PV panel with and without cooling) of $23.6 \text{ }^\circ\text{C}$ by evaporative and water circulation, which resulted in an $\approx 30\%$ of power output increment.^[60] In essence, the rate-limiting step of 2D evaporative cooling system is the vapor diffusion process, which could be addressed by increasing the evaporation surface area through creating more water/air interface. Xue et al. designed a 3D conical evaporator for room cooling (Figure 2d).^[62] Vertically aligned channels were designed in the aerogel to ensure efficient water supply by capillary effect (Figure 2e). The 3D evaporator was directly placed on the rooftop to efficiently capture heat from room, and, under one-sun illumination, the 3D evaporator reduced room temperature by $13.7 \text{ }^\circ\text{C}$, and the corresponding evaporation rate reached up to $2.23 \text{ kg m}^{-2} \text{ h}^{-1}$. Compared to the 2D evaporators, the 3D evaporators have a higher surface area, which can compensate the poor vapor diffusion in 2D evaporators, leading to their higher cooling performance.

The evaporative cooling performance of IEC is also significantly affected by the quality of water resources. Freshwater with low ion concentration is the best candidate as the precipitation of salt crystals can be avoided. However, this would limit the application of IEC only to the regions where freshwater is sufficiently available. Utilizing salt water, such as seawater and wastewater, could extend the application regions of IEC, but would suffer the problem of salt crystallization on the surface of the evaporator, which prevents vapor diffusion and leads to a lower evaporation rate. To this end, many strategies have been proposed such as designing water channel for ion diffusion back to bulk water,^[62,63] designing salt rejecting layer on evaporator,^[64,65] or isolating salt crystallization.^[65–67] Despite the great progress that has been made to utilize various liquid water for IEC, the uncompensated consumption of liquid water entails sufficient liquid water supply, which limits the application of direct evaporative cooling in the water scarcity regions.^[68]

3. Sorption-Driven Evaporative Cooling

To reduce or eliminate the reliance on liquid water for evaporative cooling, cyclic sorption-driven liquid water evaporative cooling (CSD-LWEC) and AWH-based evaporative cooling (AWH-EC) are developed. Water vapor sorbent, whose has a lower water vapor pressure at its surface than the ambient, is used to capture water vapor from its surroundings and is considered the core component of both technologies. Although sorbents are the key materials for both CSD-LWEC and AWH-EC, they have different working principles (Table 1). In CSD-LWEC, sorbent is utilized to drive water evaporation from an evaporation pond due to the low saturated vapor pressure of the sorbent, and water is regenerated by the evaporation and condensation of the adsorbed water via low-grade heat. In comparison, in AWH-EC, the sorbent is used to harvest water from atmosphere and cold is produced by evaporating the adsorbed water.^[35,69] Both approaches require the sorbents with good thermal conductivity as high thermal conductivity ensures rapid and even heat transfer across the sorbents. Fast water vapor sorption/desorption kinetics of the sorbents also help improve the performance in both approached. In addition, the AWH-EC highlights the importance of a high water uptake

Table 1. Comparison of the key features of CSD-LWEC and AWH-EC.

	CSD-LWEC	AWH-EC
High sorbent capacity	Preferred	Required
Low sorption RH	Preferred	Preferred
Fast sorption kinetics	Required	Required
Sorbent desorption temperature	Wide range	Low
High sorbent thermal conductivity	Required	Required
Energy source of sorbent desorption	Electricity or low-grade heat	Low-grade waste heat from cooling objects
System configuration	Closed system with sorbent regeneration and cooling processes separated	Opened system with sorbent regeneration and cooling processes integrated
Operational mode	Continuous cyclic mode	Discontinuous batch mode

capacity and a lower desorption temperature. The regeneration process of the sorbents in CSD-LWEC is usually separated from the cooling process, and thereby high temperature is required for higher sorbent dehydration degree and faster regeneration rate. For AWH-EC, the cooling power is generated by evaporating the water sorbed in the sorbent, driven by the waste heat from the cooling object. In such cases, a low desorption temperature is compulsory in order to maintain the cooling object at a low temperature. Meanwhile, high water uptake capacity is essential to ensure longer effective cooling duration and better cooling performance.^[42] In general, a steep water vapor uptake in a narrow humidity range is preferred since it allows water sorption at low RH while evaporating the sorbed water at a stable low temperature.^[70]

Compares some of the key features of CSD-LWEC and AWH-EC, which will be elaborated in the following sections of this review.

3.1. Cyclic Sorption-Driven Liquid Water Evaporative Cooling

3.1.1. Overview of Sorption-Driven Liquid Water Evaporative Cooling

CSD-LWEC works by removing heat from bulk water through evaporative cooling strengthened by the sorbent's sorption-desorption cycle. The evaporation-water vapor sorption process is usually a spontaneous process driven by vapor pressure gradient and barely requires additional energy input.^[30,71] In contrast, the regeneration of the sorbent necessitates the external energy input to drive the desorption of water out of the sorbent, which can be achieved by either utilizing low-grade energy (e.g., solar heating),^[72–74] or by employing high-grade energy (e.g., Joule-heating) for better sorbent regeneration degree.^[75,76]

The energy conversion and transportation in a CSD-LWEC consists of two sections. The first section is the working cycle of the system, which describes the isosteric cooling process of the sorbent after removal of its water by heating (dry sorbent) to the ambient temperature, and the isobaric sorption process

of water vapor to the dry sorbent.^[77,78] The cooled dry sorbent has a lower water vapor pressure at its surface than the water vapor pressure at the water–air interface and water vapor can be spontaneously moved from the liquid water to the sorbent. Thus, the dry sorbent is used to capture water vapor from the evaporation pond and generate cooling under constant pressure. The water vapor sorption process stops when the sorbent is saturated, which is at the point when the water vapor pressure at the sorbent and the water–air interface reaches an equilibrium. The energy extracted from the water inside the evaporation pond is equal to the total energy in this section (Figure 3a, left).^[25]

The second section is the regeneration cycle, where heating is required to release the sorbed water within the saturated sorbent (wet sorbent).^[78] When the temperature of the sorbent reaches the desorption temperature with constant pressure, the sorbed water in the sorbent can be released.^[79] The energy required for desorption of water vapor from the sorbent is equal to the total energy demand in the heating and desorption process (Figure 3a, right).^[80]

Owing to the vapor pressure differences between water and sorbents, the evaporation can take place even when the water temperature is below the ambient, thus allowing CSD-LWEC to achieve sub-ambient temperature cooling.^[81–83] Moreover, in the course of water vapor sorption processes, new hydrogen bonds among water molecules and between the water molecules and the sorbents are formed, which partially explain why these processes are typically exothermic.^[84–86] Since the cooling and the sorbent regeneration are separated in space, the cooling and heating energy can be utilized for different scenarios as cooling and heating functions with the same device (Figure 3b).^[87]

The cooling power achieved by a CSD-LWEC within an individual cooling cycle is determined by the efficiency of sorbent to extract specific amount of water from the evaporation pond.^[88,89] Thereby, the mass transport in the cooling system and water vapor sorption kinetics of the sorbent need to be optimized. In CSD-LWEC, coefficient of performance for cooling (COP_c) is used to describe the energy efficiency of the sorption-driven cooling cycle,^[77,90] which is defined as:

$$\text{COP}_c = \frac{Q_c}{W_r} \quad (2)$$

where Q_c is the cooling energy by CSD-LWEC (J), and W_r is the work required to regenerate the saturated sorbent (J). It should be mentioned that besides COP_c, temperature drop, temperature differences, and evaporation rate are also employed as performance indicators for the water-based evaporative cooling process in many other reported works. The evaporation rate determines how much energy can be taken out from the cooling media within a certain time via latent heat by evaporation-induced phase change process. The temperature drop or temperature difference reflects the degree to which the temperature of the cooling object can be reduced at specific working condition. In some cases, COP_c and the temperature drop can be interconnected. For example, a lower cooling temperature can lead to a lower COP_c of the system.^[80]

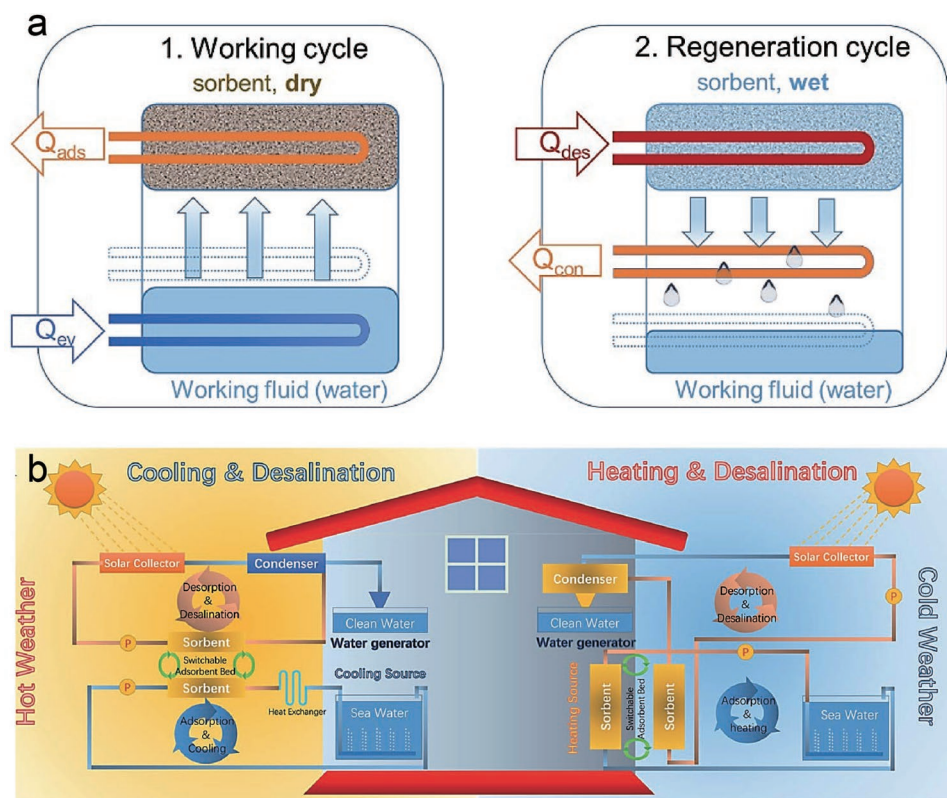


Figure 3. Schematic illustration of CSD-LWEC. a) Schematic of the operational principle of CSD-LWEC heat transformation cycle with the sorption stage (left) and the desorption stage (right). Reproduced under the terms of the CC-BY Creative Commons Attribution 3.0 Unported license (<https://creativecommons/licenses/by/3.0>).^[80] Copyright 2021, Royal Society of Chemistry. b) Schematic of the working principles of the heating and cooling processes conducted in the same CSD-LWEC device. Reproduced with permission.^[87] Copyright 2020, Royal Society of Chemistry.

3.1.2. Materials for CSD-LWEC

Solid-State Porous Sorbents for CSD-LWEC: Solid-state porous sorbent, such as silica gel, some zeolite with large pore size, have been well studied for CSD-LWEC.^[29,77,78,90,94,95] Water vapor sorption in the porous material usually experiences several steps, including single- to multilayer sorption, pore filling, and capillary condensation.^[96–98] The porous structures with abundant hydrophilic functional groups provide sufficient sorption sites with strong sorbent-water interactions for water vapor sorption, making them capable of adsorbing water vapor at low RH.^[99,100] For example, zeolite SAPO-34 is a commercially available adsorbent for CSD-LWEC.^[101,102] Based on the Young-Laplace equation,^[103–105] the microporous structure and hydrophilic nature of the SAPO-34 leads to a strong excess pressure at the meniscus of water-air interface, undesirably creating a high-energy demand for sorbent regeneration.^[106] This makes the COPc in a SAPO-34-based CSD-LWEC system only 0.68 at a regeneration temperature of 80 °C.^[91] In addition, owing to the rigid solid-state porous structure, the water uptake capacity of SAPO-34 at low RH (RH < 30%) is only 0.28 g g⁻¹.

MOFs are a series of emerging sorbent for CSD-LWEC.^[91,95,101,108,109] In particular, the MOFs with S-shaped water vapor sorption isotherms are preferable due to their ability to achieve high water uptake within a small RH window.^[98,110,111] For example, MIP-200 showed a water vapor sorption isotherm with a steep water uptake increase within

RH range of 2–20%.^[77] Its water uptake capacity was 0.39 g g⁻¹ at 25% RH and the COPc was 0.78 at a regeneration temperature of 70 °C. Lewis basic nitrogen site modified MIP-200^[91] exhibited an enhanced water uptake capacity of 0.43 g g⁻¹ at 25% RH, and the COPc was increased to 0.79 at a regeneration temperature of 70 °C (**Figure 4a**).

In addition to the chemical compositions, the pore size of the porous solid sorbents plays an important role as well.^[111–113] The critical pore diameter is defined as the pore size at which the sorption changes from continuous pore filling to hysteretic capillary condensation.^[107,108,114] Rieth et al. presented an MOF Co₂Cl₂BTDD with its pore size below the critical diameter of water ($D_c = 2.076$ nm), which successfully prevented irreversible capillary condensation at low temperature and achieved the maximal occupancy of the internal volume available for filling water (**Figure 4b**).^[92] Co₂Cl₂BTDD sorbent demonstrated a water vapor uptake capacity of 0.6 g g⁻¹ at a RH of 30%, which is 1.6 times that of Ni₂Cl₂BBTA sorbent with smaller pore diameter (i.e., 1.3 nm). The COPc of Co₂Cl₂BTDD could reach up to 0.91 at a regeneration temperature of 57 °C while Ni₂Cl₂BBTA had a COPc of 0.72 even when regenerated at 127 °C (**Figure 4c**).

Deliquescent-Salt-Based and Polymeric-Based Water Vapor Sorbents for CSD-LWEC: Deliquescent salts cover a broad range of chemicals,^[115] including but not limited to, inorganic deliquescent salts, such as lithium chloride (LiCl), calcium chloride (CaCl₂), or their mixtures. Intensive research has been performed on the deliquescent-salt-based CSD-LWEC during the

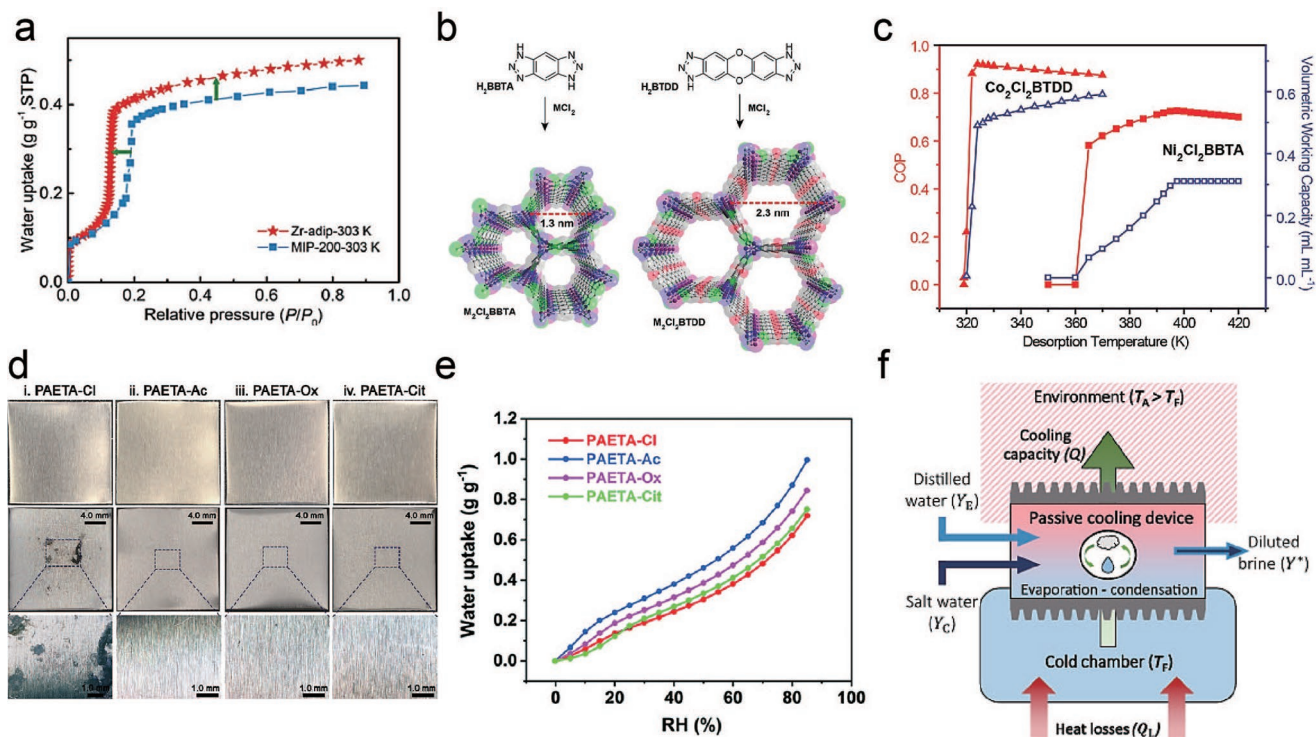


Figure 4. Water vapor sorbents for CSD-LWEC. a) Water vapor sorption isotherms of MIP-200 and modified MIP-200, featured with stepwise water vapor sorption isotherm. Reproduced under the terms of the CC-BY Creative Commons Attribution 4.0 International license (<https://creativecommons.org/licenses/by/4.0/>).^[91] Copyright 2022, The Authors, published by Wiley-VCH. b) Pore size modulation of M₂Cl₂(BTDD) MOF. c) Comparison of COPc and volume working capacity of Co₂Cl₂BTDD and Ni₂Cl₂BBTA. b,c) Reproduced with permission.^[92] Copyright 2017, American Chemical Society. d) Corrosion assessment of PAETA-X hydrogel on aluminum plates; the first row is the digital photos of pristine aluminum plates before test, the second and the third lines are the digital photos of aluminum plates after 60 days of corrosion test. e) Water vapor sorption isotherms of PAETA-X hydrogel at 25 °C, displaying a linear increase in the isotherm shapes. e,f) Reproduced with permission.^[80] Copyright 2021, Royal Society of Chemistry. f) Schematic of the working principle of passive sorption-driven cooling. Reproduced with permission.^[93] Copyright 2020, AAAS.

past years. Xiong et al. demonstrated a cooling system with a COP increment from 0.23 to 0.72 by involving a dual-staged liquid desiccant cooling system with each stage filled with different deliquescent salt (i.e., CaCl₂ and LiCl for the 1st and 2nd stage, respectively).^[116] Hassan et al. proposed a deliquescent salt mixture containing 50% of CaCl₂ and 20% CaNO₃ in their water solution, and demonstrated an improved viscosity, vapor pressure, and the heat and mass transport of the cooling system.^[117] However, the major drawbacks of deliquescent salt-based CSD-LWEC are the aqueous phase of the sorbent and their corrosivity, which complicates the design of the CSD-LWEC and increases its operational cost.^[118]

Hygroscopic polymeric sorbents (e.g., poly quaternary ammonium salts, super moist sorption gels, salt-infiltrated hydrogels.) take on quasi-solid-state, offer physical stability, and thus can be handled more easily than the deliquescent salt solution.^[81,118–124] Wang and co-workers demonstrated that incorporating deliquescent salt CaCl₂ with polymeric framework polyacrylamide (PAM) helped effectively restrain the mobility of the CaCl₂ solution.^[119] Further improvement was made by the same group to enhance the stability of the salt-polymer system by using zwitterionic polymers to replace the charge-neutral polymers in the previous works, such as polyacrylamide. The presence of the oppositely charged ions on the same polymer chains makes the zwitterionic polymers more soluble and stable in

the high concentration salt solutions, leading to a higher water vapor uptake capacity as a result of the salting-in effect.^[125] The composite of deliquescent salts with hydrogels are emerging as attractive sorbents for water-based evaporative cooling.

These group of sorbents usually experience chemisorption at the initial stage to form hydrate counterparts for salt-infiltrated hydrogels or non-freezable bonded water for pristine hygroscopic polymeric sorbents, and further liquify into high-concentration solution within the polymer framework or is softened into quasi-solid gels, respectively. Due to their expandable structures, a high water vapor uptake capacity could be achieved.^[119,125–128] Unlike the solid-state porous sorbents that rely on the physical sorption of water vapor into their porous structure and display an S-shaped water vapor sorption isotherm with a steep water uptake at specific narrow humidity range, hygroscopic polymeric-based and deliquescent-salt-based sorbents usually show a linear water uptake across a broad humidity range (shown in Figure 4a for S-shaped isotherm and Figure 4e for linear isotherm).^[124,128,129] Obviously, the water uptake capacity of the sorbents with S-shaped isotherms could be increased greatly at a small temperature variation, while linear one shows a much lower increase in water uptake capacity at the same temperature change. Moreover, moving the inflection point of the S-shaped isotherm to the low RH region would achieve high water uptake capacity at low RH, but

higher temperature will be required to release the sorbed water. However, the sorbent with a linear-shaped isotherm usually has a higher water uptake capacity at high humidity region.

One of the drawbacks of these polymeric sorbents is their slow water vapor sorption kinetics due to their dense structure and slow internal diffusivity of water molecules.^[130,131] Theoretically, reducing the size and increasing the surface area of the sorbent can be an effective approach to increase the number of the sorption sites and reduce the water molecular diffusion length, which can enhance the overall water vapor sorption kinetics.^[132–134] Wang et al. prepared a sub-micron scale sorbent consisting of LiCl and porous hollow structured SiO₂ (LiCl@SiO₂).^[87] Deliquescent salt LiCl provided superior water uptake capacity at low RH while the hollow structured SiO₂ confined the LiCl, prevented the leakage of as-formed LiCl solution, and formed a composite sorbent with high water vapor sorption kinetics (i.e., ≈4 times of pristine LiCl) and water vapor sorption capacity (i.e., 1.2 g g⁻¹) at low RH of 20%. The COP_c of LiCl@SiO₂ reached up to 0.97 at a regeneration temperature of 80 °C, which is among the best performance achieved in CSD-LWEC.

Due to the liquid features and the existence of corrosive anions Cl⁻ in most of deliquescent salts, their applications are faced with the practical challenges of easy material corrosion.^[135] Wu et al. developed a series of halide-free poly quaternary ammonium salts poly[2-(acryloyloxy)ethyl]trimethylammonium hydrogel sorbent (PAETA-X), effectively minimized the corrosion effect (Figure 4d).^[80] The water vapor uptake isotherms of the PAETA-X hydrogel sorbents showed a linear-increase along with RH. The highest water uptake capacity of the PAETA-Ac was 0.31 g g⁻¹ at 30% RH, with a COP_c of 0.75 at regeneration temperature of 70 °C (Figure 4e).

Novel CSD-LWEC system design is an alternative method to evade some deficiencies in water vapor sorbents. Alberghini et al. developed a new passive adsorption-driven cooling system that does not need complicated material design, as shown in Figure 4f.^[93] Distilled water and salt water were placed on the two sides of the hydrophobic membrane. The salinity difference would induce a vapor pressure gradient, generates a net vapor flux from the evaporating (Y_E) to the condensing (Y_C) layers, leads to the evaporation of distilled water and adsorption of water vapor in high salinity side between two inlet solutions. These evaporation–condensation processes allow the removal of heat from the lower-temperature chamber and the transfer of heat into the higher-temperature external environment. By stacking multiple same stage, the cooling performance would be enlarged, and a cooling power of 170 W m⁻² was demonstrated in a 4-stage device, in which CaCl₂ solution were used as the working fluid for water vapor sorption.

3.2. Atmospheric Water HarvestingBased Evaporative Cooling

Atmosphere preserves ≈1.2 × 10¹³ tons of fresh water.^[136,137] The efficient utilization of such ubiquitous water for different purposes has attracted numerous interests.^[138–141] Thus, extracting atmospheric water for evaporative cooling is emerging as an attractive approach in meeting global cooling demands, especially for arid and land-locked regions. AWH-EC shares similarity with CSD-LWEC, both of which require water vapor

sorbents to establish a vapor pressure gradient to drive water vapor sorption process. However, in comparison to CSD-LWEC where water is used as working fluid and the cooling and sorbent regeneration processes are separated in time, AWH-EC is different in many aspects.

In a typical AWH-EC, water vapor sorbents are directly attached to the cooling object and the sorbent sorbs and converts the atmospheric water vapor into liquid water and stores it within the sorbent. The evaporation of the stored water directly extracts heat from the hot surface until its exhaustion.^[35,42,142] Therefore, the water vapor sorption process in the AWH-EC is considered the regeneration process of the cooling system, while the cooling and the sorbent desorption processes are integrated together during operation.^[35,42,143] On the one hand, the amount of water stored in the sorbent during the cooling system regeneration process determines the duration of the stable cooling performance during the operation, which requires higher water vapor uptake capacity and water vapor sorption kinetics.^[35,42,142] On the other hand, AWH-EC is a passive cooling process, the cooling temperature that can be achieved is highly dependent on the water vapor desorption temperature of the sorbents, leading to the requirements of sorbent with low desorption temperature.

Due to the nature of the AWH-EC, the cooling process is generally performed in the open air, which allows the desorbed water vapor to effectively diffuse to the ambient air.^[35,43,142–144] With some specific design where a closed chamber was used as the condenser to encapsulate the sorbent, clean water could be produced from air with the cooling performance expectedly degraded.^[35,142] The cooling power in such design is determined by the water vapor diffusion rate and the heat dissipation performance of the condenser. It should be mentioned that the AWH-EC is still at its very early stage of development, with the amount of available literature limited.

3.2.1. Cooling Process and Cooling Power of AWH-EC

The cooling process of AWH-EC mainly consists of three different pathways, convection, radiation, and water evaporation.^[145,146]

$$\frac{Q'_c}{t} = \varphi_{\text{conv}} + \varphi_{\text{rad}} + \varphi_{\text{evap}} \quad (3)$$

where Q'_c is the energy cooled by the AWH-EC system, t is time, Q'_c/t is the cooling power of AWH-EC. φ_{conv} , φ_{rad} , and φ_{evap} are heat dissipation flux by convection, radiation, and evaporation, respectively.

$$\varphi_{\text{conv}} = hA(T_s - T_{\text{amb}}) \quad (4)$$

$$\varphi_{\text{rad}} = \sigma \varepsilon A(T_1^4 - T_{\text{amb}}^4) \quad (5)$$

$$\varphi_{\text{evap}} = m(h_w + h') \quad (6)$$

where h is convective heat transfer coefficient (W m⁻²K⁻¹), A is the contact surface area (m²) of cooling system and cooling

object, T_s and T_{amb} are the cooling object temperature and ambient temperature (K), σ is the Stefan–Boltzmann constant ($5.67 \times 10^{-8} \text{ kg s}^{-3} \text{ K}^{-4}$), ε is the emissivity coefficient of the sorbent, m is the mass of water evaporated during cooling process (g), h_v is the enthalpy of vaporization of pure water (kJ kg^{-1}), and h' is the differential enthalpy (kJ kg^{-1}) for the sorbent during the water vapor sorption process.

In general, increasing emissivity of the sorbent can enhance the cooling performance by strengthened thermal radiation.^[35,82,147] Faster evaporation rate, larger contact area, and higher thermal conductivity will help to improve heat dissipation.^[148] It is worth pointing out that the sorbent materials that have reduced enthalpy of vaporization of water are not preferred for AWH-EC as the amount of energy dissipated by evaporation of unit mass of water is declined.^[149,150] In other words, water demand is increased in such sorbent system for dissipating same amount of heat from the cooling object.

3.2.2. Materials Used for AWH-EC

Solid-State Porous Water Vapor Sorbents for AWH-EC: Porous materials such as MOFs have good water vapor capture performance at low RH and thus are also regarded as a candidate sorbent for AWH-EC. Wang et al. utilized MIL-101(Cr) as sorbent to cool down the electronic device.^[42] The water uptake capacity of the glued MIL-101(Cr) reached up to 0.92 g g^{-1} at a RH of 60%, showing an effective cooling time only 20 min at a heating power of 1.5 W ($\approx 937 \text{ W m}^{-2}$). As a result, the adsorbed water was quickly exhausted. Additionally, over 6 h were demanded to completely regenerate the sorbent at 25°C and RH of 60%. To enhance the adsorption kinetics, the use of artificial air flow on the surface of the sorbent led to the adsorption time to be shortened to less than 1 h.

The same MOF was later loaded on the carbon foam for smart battery thermal management (BTM) (Figure 5a).^[151] The prototype BTM device showed an $\approx 9^\circ \text{C}$ temperature difference after cooling at draining rate of 2.4 C .^[152] The similar concept was demonstrated by Yue et al. in a 100-battery BTM system.^[153] Furthermore, the use of MOF as sorbent in AWH-EC of mobile electronic device was reported by Wang et al., who demonstrated an extra heat dissipation capacity of $\approx 10\%$.^[142]

Polymeric-Based Water Vapor Sorbents for AWH-EC: Polymeric-based water vapor sorbents are another option for AWH-EC. The water vapor sorption process in this type of water vapor sorbents is similar to the sorption process in the liquid sorbent. The water vapor pressure gradient between the sorbent and the ambient changes quasi-linearly along with water vapor sorption until the equilibrium state is reached at the sorbent saturation.^[42] Their linearly changed water vapor sorption performance across a broad RH range makes this group of sorbents better performers at high RH, while preserving parts of their water uptake capacity at low RH.^[123,154–158] Since deliquescent salts cannot be directly used for AWH-EC due to the formation of their liquid solutions, the hybridization of hygroscopic salts and polymeric frameworks has been demonstrated a promising approach in eliminating the fluidic nature of salt solution while offering an expandable matrix to allow for a high water uptake capacity.^[119,128,131] For example,

Chen et al. developed a lithium bromine-enriched polyacrylamide hydrogel (Li-PAAm hydrogel) for semiconductor cooling (Figure 5b), in which LiBr worked as the sorbent for atmospheric water capture and PAAm hydrogel provided a solid platform that constrained the solution in a desired region.^[43] The hydrogel could reduce the cell-phone chip temperature by 15°C under the heat flux of 2229 W m^{-2} . However, effective cooling lasted for only 12 min due to the exhaustion of the sorbed water. Moreover, it required around 70 min to regenerate the sorbent by sorbing atmospheric water vapor at 25°C and RH of 70%.

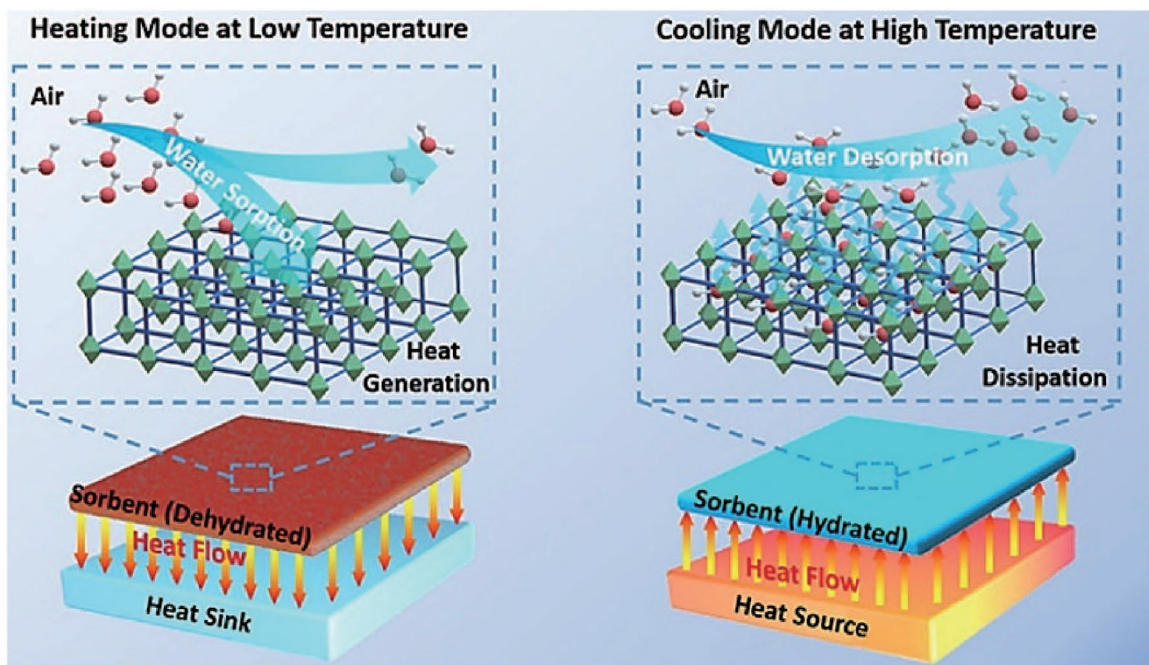
In an application scenario with lower heat flux, Wang et al. demonstrated a hygroscopic PAM-CNT- CaCl_2 hydrogel for PV cooling (Figure 6a), in which the deliquescent salt CaCl_2 worked as the sorbent.^[35,119,120,142] The water uptake capacity of the PAM-CNT- CaCl_2 hydrogel reached up to 0.99 g g^{-1} at a RH of 60%. Accordingly, the PV temperature was reduced to 45°C as compared to the solar cell working alone of 62°C under one-sun irradiation (1000 W m^{-2}). The reduced temperature of the PV increased its electricity generation by over 13%. The cooling power of the hydrogel was calculated to be 294.9 W m^{-2} . However, the solar cell temperature was increased to $\approx 54^\circ \text{C}$ by the end of the 3h illumination, which was resulted from the exhaustion of the sorbed water, emphasizing the importance of increasing water uptake capacity in order to extend the cooling effect, especially at a high heat influx.^[35] Such design was further extended to the simultaneous production of electricity, water, and crops in the desert regions, providing a proof-of-concept of AWH-cooling based hybrid system in addressing the food safety stress in arid regions.^[142]

Hygroscopic ionic liquid was also utilized as water vapor sorbent to aid cooling.^[123,159] Chen et al. developed a hydrophilic ionogel that contained poly(acrylic acid-co-2-acrylamido-2-methylpropane sulfonic acid) (P(AA-co-AMPSA)) network, hygroscopic ionic liquid of 1-ethyl-3-methylimidazolium acetate ([EMIM][Ac]) and thermal conductive reduced graphene oxide (RIG) (Figure 6b).^[144] Although, the RIG had a low water uptake capacity of 0.59 g g^{-1} at an RH of 90%, it showed an excellent adhesion performance, which could provide a stable interface and avoid mechanical deformation. Interestingly, the hydrogel could maintain a stable temperature difference of 15°C in a TEG device for over 12 h (Figure 6c), when the hot-side temperature was maintained at 50°C . The averaged evaporation rate was estimated to be $0.14 \text{ kg m}^{-2} \text{ h}^{-1}$, producing a cooling power of 91.7 W m^{-2} . Such a design is better suited where a low cooling power is expected for an elongated period of time (Table 2).

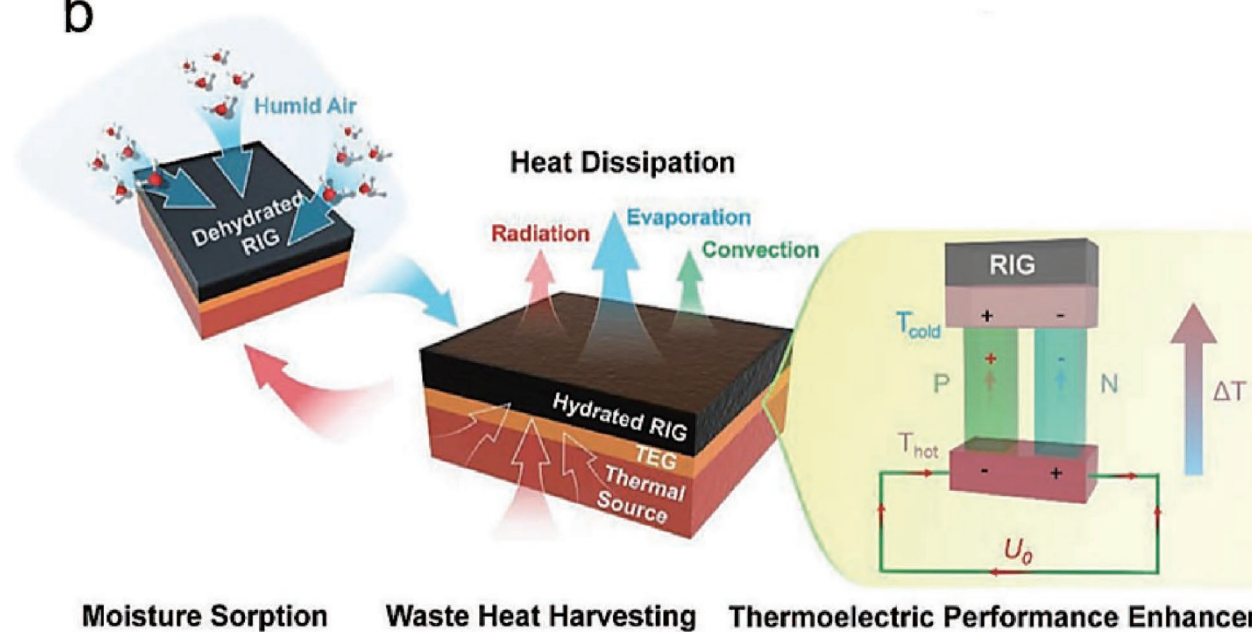
4. Conclusion and Perspective

We have summarized the recent progress in IEC, CSD-LWEC, and AWH-EC. Material engineering and structure design are typical strategies to enhance their cooling performance via enhancing thermal conductivity and evaporation rate. For example, the emergence of 3D structure could enhance the evaporation rate and cooling performance significantly, but the thermal conductivity needs to be further improved to reduce the temperature difference between the evaporation surface

a



b



Moisture Sorption

Waste Heat Harvesting

Thermoelectric Performance Enhancement

Figure 5. Water vapor sorbents for AWH-EC. a) Conceptual design of MOF@carbon foam battery thermal management system based on AWH-EC. Reproduced with permission.^[44] Copyright 2020, American Chemical Society. b) Schematic of the RIG hydrogel employed to cool down the thermoelectric generator's cold side to expand temperature differences for efficient thermoelectric performance. Reproduced with permission.^[43] Copyright 2020, Wiley-VCH.

and cooling object. For IEC, rational water channel design for water delivery from bulk water to the evaporation surface is vital to ensure efficient continuous cooling, and materials with higher internal water molecules mobility should be developed accordingly. Moreover, liquid water consumption is another

main factor that limits the development of IEC. Utilizing sea-water or wastewater is capable of mitigating its over-reliance on liquid water sources, but there still remains some challenges in multiple aspects such as salt clogging, biofouling, material stability, etc.

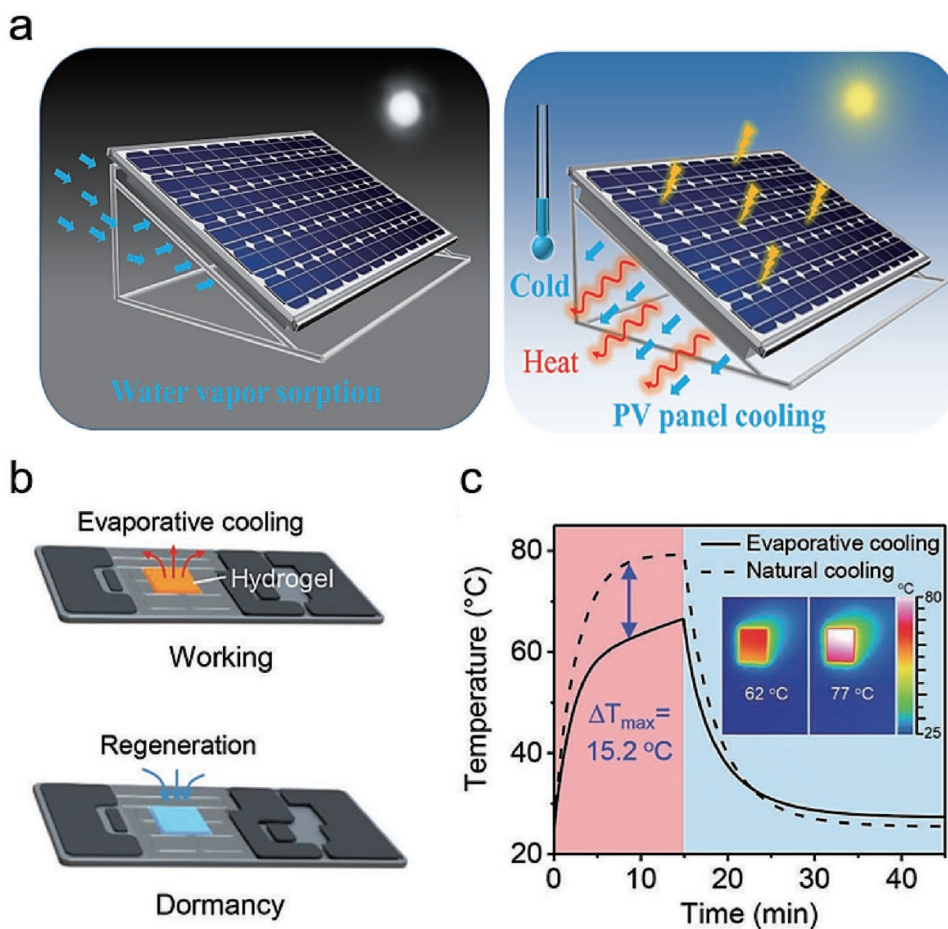


Figure 6. Application of AWH-EC in PV cooling and electronic cooling. a) Schematic illustration of the PV working with and without PAM-CNT-CaCl₂ hydrogel. Reproduced with permission.^[35] Copyright 2020, The Authors, published by Springer Nature. b) Schematics of cell-phone cooling by AWH-based evaporative cooling. c) Temperature variations of the chip with and without cooling by the hydrogel. Inset shows the infrared images of the chip with (left) and without (right) the Li-PAAm hydrogel. b,c) Reproduced with permission.^[43] Copyright 2020, Wiley-VCH.

Table 2. Summary of material properties, strategies to enhance cooling performance, and representative materials of different evaporative cooling technologies.

Cooling strategy	Key features	Representative material properties	Strategies to enhance cooling performance	Pros and cons (P and C)
IEC	1) High evaporation rate 2) Requires liquid water supply	Capillary thin-layer materials. (e.g., Cotton wick mesh, nonwoven fabric, etc.)	Material designing (composite material) Structure engineering (3D structure and aligned water channel)	P: High thermal conductivity P: Efficient heat relocation C: Massive liquid water consumption C: Limited cooling power
CSD-LWEC	1) Requires liquid water supply 2) Recycle evaporated water during operation	Solid-state porous sorbents (e.g., MOFs, COFs, etc.) Deliquescent-salt (e.g., CaCl ₂) and polymeric (e.g., PAETA-X)-based water vapor sorbents	Pore design (hydrophilicity modification, pore size modulation) Material engineering (molecular design, substrate design, system design)	P: Low sorption RH and high tunability C: Low water vapor uptake capacity P: High water vapor uptake capacity C: Slow sorption kinetics and corrosivity
AWH-EC	1) Does not require liquid water. 2) Passive heat relocation	Solid-state porous sorbents (e.g., MOFs, COFs, etc.) Polymeric-based water vapor sorbents	Structure design (substrate design) Material engineering (composite sorbent)	P: Low sorption RH, high sorption kinetics C: Rigid structure, low thermal conductivity and low water uptake capacity P: Soft and flexible structure, high thermal conductivity and high sorption capacity C: Low sorption kinetics

CSD-LWEC and AWH-EC are capable of achieving evaporative cooling without liquid water consumption. Sorbent design is of significance for both of them, but they have different requirements on sorbent properties. CSD-LWEC highlights high sorbent capacity and low sorption RH, while in addition to the above emphasis, the sorbents of AWH-EC need to have fast sorption kinetics, low desorption temperature and high thermal conductivity. Developing desired sorbents demands in-depth understanding in the interaction between sorbent and water. Moreover, since IEC and AWH-EC works in open region and the cooling power is significantly affected by the testing conditions, such as environmental temperature, humidity, heat flux, a field-accepted testing standard is urgently needed to fairly evaluate cooling power. Although, the past has witnessed commendable progresses in smart sorbent design, to date, many significant roadblocks remain, which limits the adoption of the relevant processes in practice but, at the same time, bring the new opportunities for research.

First, the rational design of the sorbent materials requires a much better understanding to the water-sorbent interaction at the molecular level. The state of water when stored inside the sorbents and its potential impacts on the water vapor sorption and desorption and the energy exchange associated with them remain ambiguous. The physicochemical properties of the sorbents in relation to water vapor sorption/desorption capacity, kinetics, and desorption temperature, among others deserve more research attentions. The fundamental knowledge, once available, will guide the design and synthesis of more advanced sorbents for a broad range of practical applications with much improved performance.

Second, the physicochemical properties of the sorbents and the cooling performance of such a system can be established, which calls for reliable system design and simulation. Such a material-properties-performance relationship would lead to the system optimization in many aspects, such as, sorbent regeneration temperature, regeneration energy demand, effective cooling duration. More specifically, focus should be made in reducing the onset sorption RH of the sorbent to reach a lower achievable cooling temperature; substrates with higher thermal conductivity should be developed and involved in the system design to support the powder-form sorbents and enhance the cooling efficiency of the evaporative cooler. Other strategies that can enhance the cooling performance such as modulating the water-sorbent interactions, requires further investigations.

Third, the CSD-LWEC and AWH-EC can be further extended to other application scenarios in energy and water sector other than cooling. On the one hand, CSD-LWEC involves phase change of water throughout the cooling process, which can be used to produce clean water from contaminated sources, such as wastewater, seawater, while simultaneously producing cooling power driven by green energy. On the other hand, current CSD-LWEC and AWH-EC can only work in an intermittent form as the sorbent needs to be regenerated, which makes them unable to provide continuous cooling. Therefore, developing novel system that is capable of generating cold continuously is highly desired, and this calls for more research efforts.

Acknowledgements

R.L. and W.W. contributed equally to this work.

Conflict of Interest

The authors declare no conflict of interest.

Keywords

atmospheric water harvesting, evaporative cooling, moisture capture, sorption-driven evaporative cooling, water vapor sorbents

Received: October 14, 2022

Revised: January 6, 2023

Published online: April 12, 2023

- [1] R. Khosla, N. D. Miranda, P. A. Trotter, A. Mazzone, R. Renaldi, C. McElroy, F. Cohen, A. Jani, R. Perera-Salazar, M. McCulloch, *Nat. Sustainability* **2021**, *4*, 201.
- [2] R. Coorey, D. S. H. Ng, V. S. Jayamanne, E. M. Buys, S. Munyard, C. J. Mousley, P. M. K. Njage, G. A. Dykes, *Compr. Rev. Food Sci. Food Saf.* **2018**, *17*, 827.
- [3] S. M. Sohel Murshed, C. A. Nieto de Castro, *Renewable Sustainable Energy Rev.* **2017**, *78*, 821.
- [4] A. Lal Basediya, D. V. K. Samuel, V. Beera, *J. Food Sci. Technol.* **2013**, *50*, 429.
- [5] H. S. Laine, J. Salpakari, E. E. Looney, H. Savin, I. M. Peters, T. J. E. Buonassisi, *Energy Environ. Sci.* **2019**, *12*, 2706.
- [6] R. Khosla, N. D. Miranda, P. A. Trotter, A. Mazzone, R. Renaldi, C. McElroy, F. Cohen, A. Jani, R. Perera-Salazar, M. J. N. S. McCulloch, *Nat. Sustainability* **2021**, *4*, 201.
- [7] L. W. Davis, P. J. Gertler, *Proc. Natl. Acad. Sci. USA* **2015**, *112*, 5962.
- [8] E. A. Goldstein, A. P. Raman, S. J. N. E. Fan, *Nat. Energy* **2017**, *2*, 17143.
- [9] J. Liu, H. Tang, C. Jiang, S. Wu, L. Ye, D. Zhao, Z. Zhou, *Adv. Funct. Mater.* **2022**, *32*, 2206962.
- [10] A. Mastrucci, E. Byers, S. Pachauri, N. D. Rao, *Energy Build.* **2019**, *186*, 405.
- [11] H. Thomson, N. Simcock, S. Bouzarovski, S. Petrova, *Energy Build.* **2019**, *196*, 21.
- [12] S. Werner, *Reference Module in Earth Systems and Environmental Sciences*, Elsevier, Amsterdam, The Netherlands **2013**.
- [13] J. Liu, J. Zhang, H. Tang, Z. Zhou, D. Zhang, L. Ye, D. Zhao, *Nano Energy* **2021**, *81*, 105611.
- [14] G. Smith, A. Gentle, *Nat. Energy* **2017**, *2*, 17142.
- [15] M. M. Hossain, M. Gu, *Adv. Sci.* **2016**, *3*, 1500360.
- [16] A. P. Raman, M. A. Anoma, L. Zhu, E. Rephaeli, S. Fan, *Nature* **2014**, *515*, 540.
- [17] J. Li, X. Wang, D. Liang, N. Xu, B. Zhu, W. Li, P. Yao, Y. Jiang, X. Min, Z. Huang, S. Zhu, S. Fan, J. Zhu, *Sci. Adv.* **2022**, *8*, eabq0411.
- [18] X. Zhilin, L. Lintao, S. Kailiang, F. Zhen, F. Xiaochun, *J. Photonics Energy* **2021**, *12*, 012113.
- [19] S. Buddhiraju, P. Santhanam, S. Fan, *Proc. Natl. Acad. Sci. USA* **2018**, *115*, E3609.
- [20] W. Wang, Y. Shi, C. Zhang, R. Li, M. Wu, S. Zhuo, S. Aleid, P. Wang, *Energy Environ. Sci.* **2022**, *15*, 136.
- [21] C. Vanderzee, D. H. Wauch, N. C. Haas, D. A. Wigg, *J. Chem. Thermodyn.* **1980**, *12*, 27.
- [22] J. R. Barbosa, G. B. Ribeiro, P. A. de Oliveira, *Heat Transfer Eng.* **2012**, *33*, 356.
- [23] X. She, L. Cong, B. Nie, G. Leng, H. Peng, Y. Chen, X. Zhang, T. Wen, H. Yang, Y. Luo, *Appl. Energy* **2018**, *232*, 157.
- [24] P. Pylysk, K. Lylykangas, J. Kurnitski, *Renewable Sustainable Energy Rev.* **2020**, *134*, 110299.

- [25] C. E. Klots, *J. Chem. Phys.* **1985**, *83*, 5854.
- [26] S. P. Fisenko, A. I. Petruichik, A. D. Solodukhin, *Int. J. Heat Mass Transfer* **2002**, *45*, 4683.
- [27] Z. Duan, C. Zhan, X. Zhang, M. Mustafa, X. Zhao, B. Alimohammadisagvand, A. Hasan, *Renewable Sustainable Energy Rev.* **2012**, *16*, 6823.
- [28] E. Schmidt, *Properties of Water and Steam in SI-Units, KJ, bar. 0-800 Degree C. 0-1000 bar*, Springer, Berlin/Heidelberg, Germany **1989**.
- [29] Y. Yang, G. Cui, C. Q. Lan, *Renewable Sustainable Energy Rev.* **2019**, *113*, 109230.
- [30] P. M. Cuce, S. Riffat, *Renewable Sustainable Energy Rev.* **2016**, *54*, 1240.
- [31] S. Fisenko, A. Brin, A. Petruichik, *Int. J. Heat Mass Transfer* **2004**, *47*, 165.
- [32] K. M. Bataineh, S. Alrifai, *Adv. Mech. Eng.* **2015**, *7*, 168781401558612.
- [33] R. Kühn, J. Römer, F. Ziegler, *Int. J. Refrig.* **2018**, *95*, 133.
- [34] E. Laurenz, G. Földner, L. Schnabel, G. Schmitz, *Energies* **2020**, *13*, 3003.
- [35] R. Li, Y. Shi, M. Wu, S. Hong, P. Wang, *Nat. Sustainability* **2020**, *3*, 636.
- [36] Y. Tu, R. Wang, Y. Zhang, J. Wang, *Joule* **2018**, *2*, 1452.
- [37] X. Zhou, H. Lu, F. Zhao, G. Yu, *ACS Mater. Lett.* **2020**, *2*, 671.
- [38] *Oxford English Dictionary*, Simpson, Ja, Weiner, Esc. **1989**, *3*.
- [39] T. Miyazaki, A. Akisawa, I. Nikai, *Energy Build.* **2011**, *43*, 2211.
- [40] M. Mujahid Rafique, P. Gandhidasan, S. Rehman, L. M. Al-Hadhrani, *Renewable Sustainable Energy Rev.* **2015**, *45*, 145.
- [41] R. Z. Wang, R. G. Oliveira, *Prog. Energy Combust. Sci.* **2006**, *32*, 424.
- [42] C. Wang, L. Hua, H. Yan, B. Li, Y. Tu, R. Wang, *Joule* **2020**, *4*, 435.
- [43] S. Pu, J. Fu, Y. Liao, L. Ge, Y. Zhou, S. Zhang, S. Zhao, X. Liu, X. Hu, K. Liu, J. Chen, *Adv. Mater.* **2020**, *32*, 1907307.
- [44] U. Sajjad, N. Abbas, K. Hamid, S. Abbas, I. Hussain, S. M. Ammar, M. Sultan, H. M. Ali, M. Hussain, C. C. Wang, *Int. Commun. Heat Mass Transfer* **2021**, *122*, 105140.
- [45] H. Yang, W. Shi, Y. Chen, Y. Min, *Renewable Sustainable Energy Rev.* **2021**, *145*, 111082.
- [46] Y. Fang, X. Zhao, G. Chen, T. Tat, J. Chen, *Joule* **2021**, *5*, 752.
- [47] M. Yan, S. He, M. Gao, M. Xu, J. Miao, X. Huang, K. Hooman, *Int. J. Refrig.* **2021**, *121*, 23.
- [48] A. H. Alami, *Energy Convers. Manage.* **2014**, *77*, 668.
- [49] M. Chandrasekar, S. Suresh, T. Senthilkumar, M. Ganesh Karthikeyan, *Energy Convers. Manage.* **2013**, *71*, 43.
- [50] X. Li, W. Xie, J. Zhu, *Adv. Sci.* **2022**, *9*, 2104181.
- [51] Z. Liu, Z. Zhou, N. Wu, R. Zhang, B. Zhu, H. Jin, Y. Zhang, M. Zhu, Z. Chen, *ACS Nano* **2021**, *15*, 13007.
- [52] Z. Yu, R. Gu, Y. Tian, P. Xie, B. Jin, S. Cheng, *Adv. Funct. Mater.* **2022**, *32*, 2108586.
- [53] Q.-F. Guan, Z.-M. Han, Z.-C. Ling, H.-B. Yang, S.-H. Yu, *Nano Lett.* **2020**, *20*, 5699.
- [54] J. Li, X. Wang, Z. Lin, N. Xu, X. Li, J. Liang, W. Zhao, R. Lin, B. Zhu, G. Liu, L. Zhou, S. Zhu, J. Zhu, *Joule* **2020**, *4*, 928.
- [55] Y. Shi, R. Li, Y. Jin, S. Zhuo, L. Shi, J. Chang, S. Hong, K. C. Ng, P. Wang, *Joule* **2018**, *2*, 1171.
- [56] X. Wu, Z. Wu, Y. Wang, T. Gao, Q. Li, H. Xu, *Adv. Sci.* **2021**, *8*, 2002501.
- [57] Y. Wang, X. Wu, T. Gao, Y. Lu, X. Yang, G. Y. Chen, G. Owens, H. Xu, *Nano Energy* **2021**, *79*, 105477.
- [58] S. Zheng, M. Yang, X. Chen, C. E. White, L. Hu, Z. J. Ren, *Environ. Sci. Technol.* **2022**, *56*, 1289.
- [59] N. Xu, P. Zhu, Y. Sheng, L. Zhou, X. Li, H. Tan, S. Zhu, J. Zhu, *Joule* **2020**, *4*, 347.
- [60] W. Wang, S. Aleid, Y. Shi, C. Zhang, R. Li, M. Wu, S. Zhuo, P. Wang, *Joule* **2021**, *5*, 1873.
- [61] E. B. Agyekum, S. PraveenKumar, N. T. Alwan, V. I. Velkin, S. E. Shcheklein, *Heliyon* **2021**, *7*, e07920.
- [62] J. Tang, Z. Song, X. Lu, N. Li, L. Yang, T. Sun, Y. Wang, Y. Shao, H. Liu, G. Xue, *Chem. Eng. J.* **2022**, *429*, 132089.
- [63] N. Xu, J. Li, Y. Wang, C. Fang, X. Li, Y. Wang, L. Zhou, B. Zhu, Z. Wu, S. Zhu, J. Zhu, *Sci. Adv.* **2019**, *5*, eaaw7013.
- [64] W. Zhao, H. Gong, Y. Song, B. Li, N. Xu, X. Min, G. Liu, B. Zhu, L. Zhou, X.-X. Zhang, J. Zhu, *Adv. Funct. Mater.* **2021**, *31*, 2100025.
- [65] L. Li, N. He, B. Jiang, K. Yu, Q. Zhang, H. Zhang, D. Tang, Y. Song, *Adv. Funct. Mater.* **2021**, *31*, 2104380.
- [66] Y. Shi, C. Zhang, R. Li, S. Zhuo, Y. Jin, L. Shi, S. Hong, J. Chang, C. Ong, P. Wang, *Environ. Sci. Technol.* **2018**, *52*, 11822.
- [67] Y. Xia, Q. Hou, H. Jubaer, Y. Li, Y. Kang, S. Yuan, H. Liu, M. W. Woo, L. Zhang, L. Gao, H. Wang, X. Zhang, *Energy Environ. Sci.* **2019**, *12*, 1840.
- [68] C. A. Dieter, Estimated Use of Water in the United States in 2015, Geological Survey **2018**, <https://doi.org/10.3133/cir1441>.
- [69] O. Amer, R. Boukhanouf, H. Ibrahim, *Int. J. Environ. Sci. Dev.* **2015**, *6*, 111.
- [70] Z. Chen, S. Song, B. Ma, Y. Li, Y. Shao, J. Shi, M. Liu, H. Jin, D. Jing, *Sol. Energy Mater. Sol. Cells* **2021**, *230*, 111233.
- [71] A. Khandelwal, P. Talukdar, S. Jain, *Energy Build.* **2011**, *43*, 581.
- [72] X. Q. Zhai, R. Z. Wang, *Renewable Sustainable Energy Rev.* **2009**, *13*, 1523.
- [73] L. A. Chidambaram, A. S. Ramana, G. Kamaraj, R. Velraj, *Renewable Sustainable Energy Rev.* **2011**, *15*, 3220.
- [74] G. Grossman, A. Johannsen, *Prog. Energy Combust. Sci.* **1981**, *7*, 185.
- [75] D. La, Y. J. Dai, Y. Li, Z. Y. Tang, T. S. Ge, R. Z. Wang, *Appl. Energy* **2013**, *102*, 1218.
- [76] İ. Uçkan, T. Yılmaz, E. Hürdoğan, O. Büyükalaca, *Energy Convers. Manage.* **2013**, *65*, 606.
- [77] S. Wang, J. S. Lee, M. Wahiduzzaman, J. Park, M. Muschi, C. Martineau-Corcus, A. Tissot, K. H. Cho, J. Marrot, W. Shepard, *Nat. Energy* **2018**, *3*, 985.
- [78] M. F. de Lange, K. J. F. M. Verouden, T. J. H. Vlugt, J. Gascon, F. Kapteijn, *Chem. Rev.* **2015**, *115*, 12205.
- [79] H. Cao, B. Liu, L. Qin, *Appl. Therm. Eng.* **2022**, *213*, 118680.
- [80] M. Wu, R. Li, Y. Shi, M. Altunkaya, S. Aleid, C. Zhang, W. Wang, P. Wang, *Mater. Horiz.* **2021**, *8*, 1518.
- [81] A. Aili, X. Yin, R. Yang, *Appl. Therm. Eng.* **2022**, *202*, 117909.
- [82] Z. Lu, A. Leroy, L. Zhang, J. J. Patil, E. N. Wang, J. C. Grossman, *Cell Rep. Phys. Sci.* **2022**, *3*, 101068.
- [83] B. Zhao, X. Yue, Q. Tian, F. Qiu, Y. Li, T. Zhang, *Cellulose* **2022**, *29*, 7775.
- [84] Y. Cui, S. Gao, R. Zhang, L. Cheng, J. Yu, *Polymers* **2020**, *12*, 98.
- [85] P. Grönquist, M. Frey, T. Keplinger, I. Burgert, *ACS Omega* **2019**, *4*, 12425.
- [86] S. S. Barton, M. J. B. Evans, J. A. F. MacDonald, *Carbon* **1991**, *29*, 1099.
- [87] K. Yang, Y. Shi, M. Wu, W. Wang, Y. Jin, R. Li, M. Wakil Shahzad, K. Choon Ng, P. Wang, *J. Mater. Chem. A* **2020**, *8*, 1887.
- [88] G. Heidarinejad, M. Bozorgmehr, S. Delfani, J. Esmaeelian, *Build. Environ.* **2009**, *44*, 2073.
- [89] T. Wang, C. Sheng, A. G. A. Nnanna, *Energy Build.* **2014**, *81*, 435.
- [90] L. Garzón-Tovar, J. Pérez-Carvajal, I. Imaz, D. Maspoch, *Adv. Funct. Mater.* **2017**, *27*, 1606424.
- [91] B. Li, F.-F. Lu, X.-W. Gu, K. Shao, E. Wu, G. Qian, *Adv. Sci.* **2022**, *9*, 2105556.
- [92] A. J. Rieth, S. Yang, E. N. Wang, M. Dincă, *ACS Cent. Sci.* **2017**, *3*, 668.
- [93] M. Alberghini, M. Morciano, M. Fasano, F. Bertiglia, V. Fericola, P. Asinari, E. Chiavazzo, *Sci. Adv.* **2020**, *6*, eaax5015.
- [94] K. H. Cho, D. D. Borges, U. H. Lee, J. S. Lee, J. W. Yoon, S. J. Cho, J. Park, W. Lombardo, D. Moon, A. Sapienza, G. Maurin, J.-S. Chang, *Nat. Commun.* **2020**, *11*, 5112.
- [95] C. Y. Tso, K. C. Chan, C. Y. H. Chao, C. L. Wu, *Int. J. Heat Mass Transfer* **2015**, *85*, 343.

- [96] K. Yang, T. Pan, Q. Lei, X. Dong, Q. Cheng, Y. Han, *Environ. Sci. Technol.* **2021**, *55*, 6542.
- [97] H. Furukawa, F. Gándara, Y.-B. Zhang, J. Jiang, W. L. Queen, M. R. Hudson, O. M. Yaghi, *J. Am. Chem. Soc.* **2014**, *136*, 4369.
- [98] X. Liu, X. Wang, F. Kapteijn, *Chem. Rev.* **2020**, *120*, 8303.
- [99] H. Kim, S. R. Rao, E. A. Kapustin, L. Zhao, S. Yang, O. M. Yaghi, E. N. Wang, *Nat. Commun.* **2018**, *9*, 1191.
- [100] H. Kim, S. Yang, S. R. Rao, S. Narayanan, E. A. Kapustin, H. Furukawa, A. S. Umans, O. M. Yaghi, E. N. Wang, *Science* **2017**, *356*, 430.
- [101] A. Freni, L. Bonaccorsi, L. Calabrese, A. Capri, A. Frazzica, A. Sapienza, *Appl. Therm. Eng.* **2015**, *82*, 1.
- [102] Y. Liu, Z. Yuan, X. Wen, C. Du, *Appl. Therm. Eng.* **2021**, *182*, 116019.
- [103] A. F. Stalder, T. Melchior, M. Müller, D. Sage, T. Blu, M. Unser, *Colloids Surf., A* **2010**, *364*, 72.
- [104] T. Young, *Philos. Trans. R. Soc. London* **1805**, *95*, 65.
- [105] P.-S. Laplace, *Théorie de l'action capillaire—Supplément au dixième livre du traité de mécanique céleste*, Courcier, Paris, France **1806**.
- [106] T. Tsuru, T. Hino, T. Yoshioka, M. Asaeda, *J. Membr. Sci.* **2001**, *186*, 257.
- [107] N. Hanikel, X. Pei, S. Chhedha, H. Lyu, W. Jeong, J. Sauer, L. Gagliardi, O. M. Yaghi, *Science* **2021**, *374*, 454.
- [108] M. J. Kalmutzki, C. S. Diercks, O. M. Yaghi, *Adv. Mater.* **2018**, *30*, 1704304.
- [109] A. J. Rieth, A. M. Wright, G. Skorupskii, J. L. Mancuso, C. H. Hendon, M. Dincă, *J. Am. Chem. Soc.* **2019**, *141*, 13858.
- [110] Y.-Z. Zhang, T. He, X.-J. Kong, X.-L. Lv, X.-Q. Wu, J.-R. Li, *ACS Appl. Mater. Interfaces* **2018**, *10*, 27868.
- [111] J. Hagymassy, S. Brunauer, R. S. Mikhail, *J. Colloid Interface Sci.* **1969**, *29*, 485.
- [112] N. J. Foley, K. M. Thomas, P. L. Forshaw, D. Stanton, P. R. Norman, *Langmuir* **1997**, *13*, 2083.
- [113] A. W. Harding, N. J. Foley, P. R. Norman, D. C. Francis, K. M. Thomas, *Langmuir* **1998**, *14*, 3858.
- [114] H. Lu, W. Shi, Y. Guo, W. Guan, C. Lei, G. Yu, *Adv. Mater.* **2022**, *34*, 2110079.
- [115] N. Fumo, D. Y. Goswami, *Sol. Energy* **2002**, *72*, 351.
- [116] Z. Q. Xiong, Y. J. Dai, R. Z. Wang, *Appl. Energy* **2010**, *87*, 1495.
- [117] A. A. M. Hassan, M. S. Hassan, *Renewable Energy* **2008**, *33*, 1989.
- [118] R. Li, Y. Shi, L. Shi, M. Alsaedi, P. Wang, *Environ. Sci. Technol.* **2018**, *52*, 5398.
- [119] R. Li, Y. Shi, M. Alsaedi, M. Wu, L. Shi, P. Wang, *Environ. Sci. Technol.* **2018**, *52*, 11367.
- [120] R. Li, M. Wu, Y. Shi, S. Aleid, W. Wang, C. Zhang, P. Wang, *J. Mater. Chem. A* **2021**, *9*, 14731.
- [121] Y. Hu, Z. Fang, X. Ma, X. Wan, S. Wang, S. Fan, Z. Ye, X. Peng, *Appl. Mater. Today* **2021**, *23*, 101076.
- [122] X. Wang, D. Yang, M. Zhang, Q. Hu, K. Gao, J. Zhou, Z.-Z. Yu, *ACS Appl. Mater. Interfaces* **2022**, *14*, 33881.
- [123] X. Wang, X. Li, G. Liu, J. Li, X. Hu, N. Xu, W. Zhao, B. Zhu, J. Zhu, *Angew. Chem., Int. Ed.* **2019**, *58*, 12054.
- [124] F. Zhao, X. Zhou, Y. Liu, Y. Shi, Y. Dai, G. Yu, *Adv. Mater.* **2019**, *31*, 1806446.
- [125] S. Aleid, M. Wu, R. Li, W. Wang, C. Zhang, L. Zhang, P. Wang, *ACS Mater. Lett.* **2022**, *4*, 511.
- [126] R. S. Dassanayake, N. Renuka, *Adv. Technol.* **2021**, *1*, <https://doi.org/10.31357/ait.v1i1.4977>.
- [127] C. Lei, Y. Guo, W. Guan, H. Lu, W. Shi, G. Yu, *Angew. Chem., Int. Ed.* **2022**, *61*, e202200271.
- [128] P. A. Kallenberger, M. Fröba, *Commun. Chem.* **2018**, *1*, 28.
- [129] H. Mittal, A. Al Alili, S. M. Alhassan, *Colloids Surf., A* **2020**, *599*, 124813.
- [130] H. Zhu, R. Li, H. Guo, *Matter* **2022**, *5*, 2578.
- [131] J. Wang, C. Deng, G. Zhong, W. Ying, C. Li, S. Wang, Y. Liu, R. Wang, H. Zhang, *Cell Rep. Phys. Sci.* **2022**, *3*, 100954.
- [132] R. Li, Y. Shi, M. Wu, S. Hong, P. Wang, *Nano Energy* **2020**, *67*, 104255.
- [133] H. Park, I. Haechler, G. Schnoering, M. D. Ponte, T. M. Schutzius, D. Poulidakos, *ACS Appl. Mater. Interfaces* **2022**, *14*, 2237.
- [134] W. Shi, W. Guan, C. Lei, G. Yu, *Angew. Chem., Int. Ed.* **2022**, *61*, e202211267.
- [135] G. S. Frankel, J. D. Vienna, J. Lian, J. R. Scully, S. Gin, J. V. Ryan, J. Wang, S. H. Kim, W. Windl, J. Du, *npj Mater. Degrad* **2018**, *2*, 15.
- [136] S. H. Schneider, *Encyclopedia of Climate and Weather*, Vol. 1, Oxford University Press, Oxford, UK **2011**.
- [137] J. Lord, A. Thomas, N. Treat, M. Forkin, R. Bain, P. Dulac, C. H. Behroozi, T. Mamutov, J. Fongheiser, N. Kobilansky, S. Washburn, C. Truesdell, C. Lee, P. H. Schmaelzle, *Nature* **2021**, *598*, 611.
- [138] Y. Zhang, D. K. Nandakumar, S. C. Tan, *Joule* **2020**, *4*, 2532.
- [139] X. Liu, H. Gao, J. E. Ward, X. Liu, B. Yin, T. Fu, J. Chen, D. R. Lovley, J. Yao, *Nature* **2020**, *578*, 550.
- [140] L. Yang, S. K. Ravi, D. K. Nandakumar, F. I. Alzakia, W. Lu, Y. Zhang, J. Yang, Q. Zhang, X. Zhang, S. C. Tan, *Adv. Mater.* **2019**, *31*, 1902963.
- [141] J. Yang, X. Zhang, H. Qu, Z. G. Yu, Y. Zhang, T. J. Eey, Y.-W. Zhang, S. C. Tan, *Adv. Mater.* **2020**, *32*, 2002936.
- [142] H. R. Liu, C. X. Wang, B. J. Li, L. J. Hua, J. Q. Yu, R. Z. Wang, *Mater. Today Nano* **2022**, *18*, 100198.
- [143] S. Pu, Y. Liao, K. Chen, J. Fu, S. Zhang, L. Ge, G. Conta, S. Bouzarif, T. Cheng, X. Hu, K. Liu, J. Chen, *Nano Lett.* **2020**, *20*, 3791.
- [144] F. Ni, P. Xiao, C. Zhang, W. Zhou, D. Liu, S.-W. Kuo, T. Chen, *Adv. Mater.* **2021**, *33*, 2103937.
- [145] F. P. Incropera, D. P. DeWitt, T. L. Bergman, A. S. Lavine, *Fundamentals of Heat and Mass Transfer*, Vol. 6, Wiley, New York **1996**.
- [146] M. J. Moran, H. N. Shapiro, D. D. Boettner, M. B. Bailey, *Fundamentals of Engineering Thermodynamics*, John Wiley & Sons, Hoboken, NJ, USA **2010**.
- [147] L. Xu, D.-W. Sun, Y. Tian, L. Sun, T. Fan, Z. Zhu, *ACS Appl. Mater. Interfaces* **2022**, *14*, 45788.
- [148] A. LaPotin, H. Kim, S. R. Rao, E. N. Wang, *Acc. Chem. Res.* **2019**, *52*, 1588.
- [149] X. Zhou, F. Zhao, Y. Guo, B. Rosenberger, G. Yu, *Sci. Adv.* **2019**, *5*, eaaw5484.
- [150] F. Zhao, X. Zhou, Y. Shi, X. Qian, M. Alexander, X. Zhao, S. Mendez, R. Yang, L. Qu, G. Yu, *Nat. Nanotechnol.* **2018**, *13*, 489.
- [151] J. Xu, J. Chao, T. Li, T. Yan, S. Wu, M. Wu, B. Zhao, R. Wang, *ACS Cent. Sci.* **2020**, *6*, 1542.
- [152] F. Wang, N. Xu, J. Zhu, *ACS Cent. Sci.* **2020**, *6*, 1479.
- [153] Q. L. Yue, C. X. He, J. Sun, J. B. Xu, T. S. Zhao, *Appl. Therm. Eng.* **2022**, *207*, 118156.
- [154] K. Matsumoto, N. Sakikawa, T. Miyata, *Nat. Commun.* **2018**, *9*, 2315.
- [155] F. Ni, N. Qiu, P. Xiao, C. Zhang, Y. Jian, Y. Liang, W. Xie, L. Yan, T. Chen, *Angew. Chem., Int. Ed.* **2020**, *59*, 19237.
- [156] Y. Byun, A. Coskun, *Angew. Chem., Int. Ed.* **2018**, *57*, 3173.
- [157] H. Qi, T. Wei, W. Zhao, B. Zhu, G. Liu, P. Wang, Z. Lin, X. Wang, X. Li, X. Zhang, J. Zhu, *Adv. Mater.* **2019**, *31*, 1903378.
- [158] J. Xu, T. Li, J. Chao, S. Wu, T. Yan, W. Li, B. Cao, R. Wang, *Angew. Chem., Int. Ed.* **2020**, *59*, 5202.
- [159] Y. Chen, X. Sun, C. Yan, Y. Cao, T. Mu, *J. Phys. Chem. B* **2014**, *118*, 11523.